

Crossed-beam measurements of differential cross sections for elastic scattering and charge exchange in low-energy Ar^+ -Ar collisions

M. L. Vestal,* C. R. Blakley,* and J. H. Futrell

Department of Chemistry, University of Utah, Salt Lake City, Utah 84112

(Received 12 October 1977)

Differential cross sections for Ar^+ -Ar collisions have been measured at four laboratory energies in the range 2.7–20 eV and laboratory scattering angles from 2 to 90 deg using a crossed-beam apparatus. Data are presented as absolute differential cross sections in the center-of-mass coordinate system as functions of relative translational energy and center-of-mass scattering angle. The data presented should be sufficient to allow rather precise determination of the long-range portion of the Ar^+ -Ar interaction potentials. Preliminary interpretation of the rainbow scattering data gives a dissociation energy D_e for the $^2\Sigma_u^+$ state of Ar_2^+ of 1.40 ± 0.05 eV.

I. INTRODUCTION

Renewed interest in the potential curves of rare-gas dimer ions has been stimulated by recent demonstrations of vacuum-uv lasers involving Rydberg states of the neutral molecules.¹ Since these states may be described by a single electron in an outer orbit of the diatomic ion,² knowledge of the ionic molecular states is basic to an understanding of the excimer states. Earlier measurements of elastic scattering of Ar^+ -Ar have been reported by Lorents and co-workers^{3,4} and by Mittmann and Weise.⁵ Recently, several new experimental methods have been applied to studies of the Ar_2^+ system. Photoionization efficiency measurements on the Ar_2 Van der Waals dimer, using a molecular-beam technique, were reported recently by Ng, Trevor, Mahan, and Lee.⁶ Measurements of photodissociation cross sections for Ar_2^+ have been reported by Miller, Ling, Saxon, and Moseley⁷ and by Vestal and Mauclair.⁸ Moseley and co-workers⁹ have reported an extensive study of the Ar_2^+ potential curves using the technique of photofragment spectroscopy.

In the present work, we have repeated the earlier Ar^+ -Ar scattering experiments at laboratory energies of 10 and 20 eV, but have extended the angular range out to 90° in the laboratory, and have also measured the differential cross sections for elastic scattering and charge exchange at lower energies. As discussed in connection with our earlier work on He^+ -He scattering,¹⁰ measurements at low energies which include differential cross sections for charge exchange should allow a more precise determination of structural features in the scattering, such as the rainbow maximum, and, correspondingly, a more precise determination of the potentials.

The experimental apparatus and techniques employed in this work are identical to those described previously,¹⁰ with one exception. For the

present work, the Ar neutral beam was formed by a seeded supersonic molecular beam with H_2 as the carrier. This technique has the advantage that the neutral energy is substantially increased, moving it to a more convenient energy in the laboratory; however, it has the disadvantage that the absolute spread in energy of the neutral beam is substantially increased, causing some loss of effective resolution in the wide-angle scattering measurements. The use of the seeded beam also introduces an added uncertainty in the determination of absolute cross sections since the intensity of the Ar portion of the neutral beam is more difficult to determine with good absolute accuracy.

II. EXPERIMENTAL

The argon neutral beam was formed using a mixture of 7.8% Ar in H_2 . For the fully expanded supersonic jet, the most probable axial velocity is given by

$$v = (5kT/\bar{m})^{1/2}, \quad (1)$$

where T is the stagnation temperature, k is Boltzmann's constant and \bar{m} is the average mass of the molecules in the jet.¹¹ For this mixture, \bar{m} is 4.96 amu and the most probable velocity ($T = 300$ K) is 1.59×10^5 cm/sec. Assuming no slippage between the argon and hydrogen, the calculated energy of the Ar neutrals is 0.52 eV.

The energy distribution of the neutral beam was measured by ionizing a small fraction with an intersecting electron beam and measuring the energy distribution of the resulting ions with the ion analyzer set at 90° in the laboratory. The measured distribution is shown in Fig. 1, and, as shown in the figure, the most-probable energy determined experimentally is 0.53 eV. The full width at half maximum is 0.20 eV. Since the calculated full width at half maximum of the transmission function for the energy analyzer under

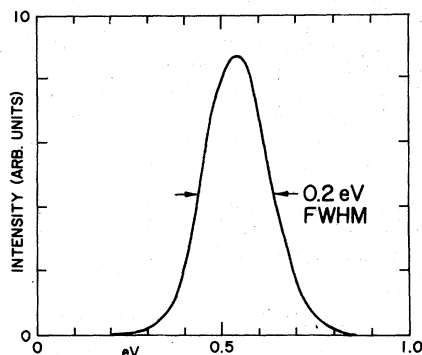


FIG. 1. Energy distribution of the Ar neutral beam determined by ionizing a portion of the beam with an intersecting electron beam and using the ion analyzer set in line with the axis of the neutral beam.

the conditions of this measurement is only about 0.07 eV, the measured distribution is not significantly different from the true energy distribution of the Ar neutrals.¹²

The response of the neutral-beam detector was calibrated independently for beams of pure argon and pure hydrogen, but was not calibrated directly for the seeded beam. The enrichment of the heavy species in a supersonic expansion is given approximately by the mass ratio.¹¹ Thus, for the conditions employed in this work, the beam composition was approximately 62% argon and the balance H₂. The response of the beam detector to a beam of this composition was calculated from the calibration factors for the pure gases. For the present work, the Ar neutral-beam intensity obtained by this procedure was 2.3×10^{15} molecules/sec with an estimated uncertainty of $\pm 20\%$.

The properties of the ion beams employed in these experiments are summarized in Table I. The ion-beam intensities were substantially greater than used in the He⁺-He work described previously¹⁰ which caused a small amount of space-charge broadening as shown by the slightly larger

TABLE I. Summary of primary-ion-beam characteristics.

Laboratory energy (eV)	Angular width ^a		Diameter ^d (cm)	Intensity (10 ⁻¹⁰ A)
	Total ^b	Beam ^c		
19.9	0.55	0.3	0.37	8.4
10.7	0.55	0.3	0.37	5.7
5.1	0.65	0.5	0.38	2.0
2.23	1.85	1.8	0.42	3.9

^a Half width at half maximum in degrees.

^b Measured width.

^c Estimated after correction for detector resolution according to Eq. (12) of Ref. 6.

^d Calculated from Eq. (13) of Ref. 6.

beam diameters and angular divergences compared to the He⁺ beam at comparable energies. Ion-beam energy distributions were recorded at each energy and the results were essentially the same as found for the He⁺ beams. All of the other instrumental parameters and distributions were identical with those described in detail in our earlier work,¹⁰ and the same techniques and computer programs were used to obtain absolute differential cross sections from the measured intensities of scattered ions.

III. RESULTS AND DISCUSSION

The differential-cross-section data obtained in this work are summarized in Figs. 2 (a)–2(d). The data are presented as semilog plots of absolute differential cross section per steradian in the center-of-mass coordinate frame. In this representation, the reactant ion is at 0° and the reactant neutral at 180°. These plots are direct tracings of computer plots drawn by the data-reduction computer program. The data points are connected by straight-line segments to aid in visualization. The error bars indicate \pm one standard deviation as determined from counting statistics; where error bars are not visible the calculated error was smaller than the size of the plotted points. Our worst-case estimate of the probable error in the absolute cross section is $\pm 40\%$; however, the error in the relative cross sections is much smaller, both between runs and within a single run, and is probably not greater than $\pm 10\%$. Near either of the reactant beams the angular uncertainty is $\pm 0.2^\circ$; however, at angles near 90° (center-of-mass), this uncertainty may be as large as $\pm 0.5^\circ$.

Our results at a relative collision energy of 10 eV are compared with the earlier work of Aberth and Lorents³ in Fig. 3. While the two results are in fairly good agreement, the discrepancies that are observed are very similar to those found between our results¹⁰ and those of Lorents and Aberth¹³ for the He⁺-He system. In every case our absolute cross sections are smaller by a factor of 2 to 3 and corresponding structural features in the cross-section curves are found at somewhat larger scattering angles in our work.

Our results for the three higher energies are shown plotted in reduced coordinates, $\tau = E\chi$ and $\rho = 2\pi\chi \sin\chi d\sigma/d\Omega$, in Fig. 4. Part (a) shows the results in the "elastic" scattering region extending from the ion beam to somewhat beyond the rainbow angle, and part (b) is the corresponding data in the "charge exchange" region with χ replaced by $\pi - \chi$ in computing the reduced variables. In all six curves, the rainbow maximum

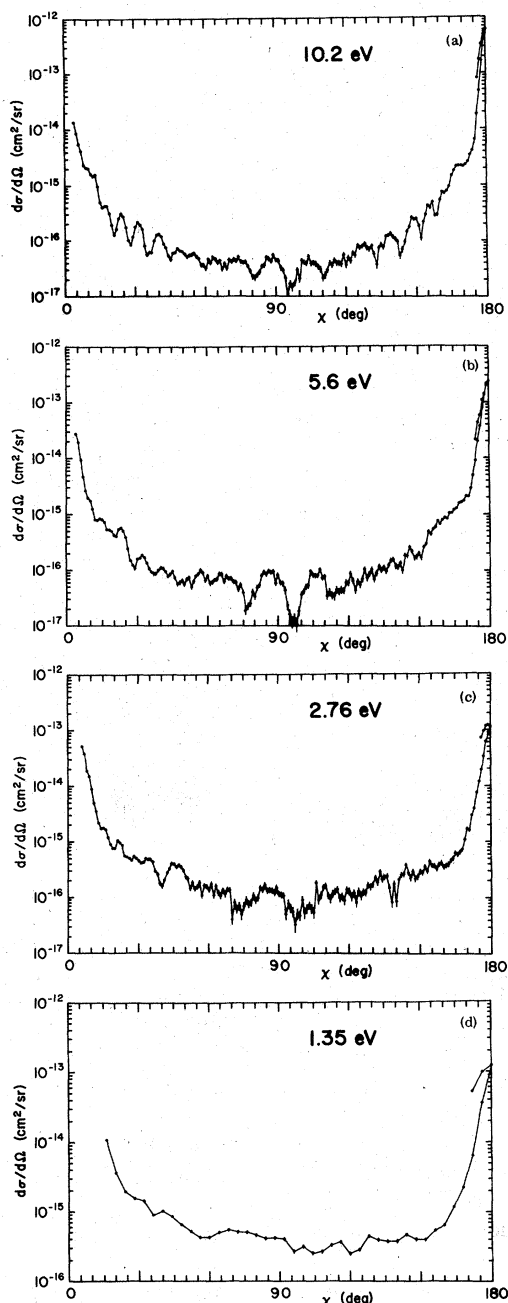


FIG. 2. (a)–(d) Absolute differential cross sections for $\text{Ar}^+ - \text{Ar}$ scattering determined in the present work. Data are presented in center-of-mass coordinates. The relative translational energy is indicated on each plot.

is clearly visible and occurs at $\tau = 130 \pm 2$ eV deg. From theoretical considerations it is expected that the position of the rainbow maximum, as a function of τ , should be nearly independent of energy. Lorents *et al.*⁴ found a smaller value of $\tau = 115$ eV deg for the rainbow angle in reduced

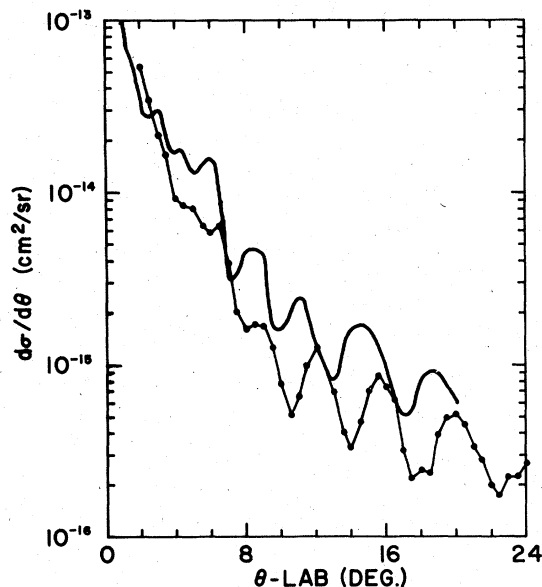


FIG. 3. Comparison of present results at 10 eV relative collision energy with the earlier work of Aberth and Lorents (Ref. 3).

coordinates with the value varying from about 124 eV deg at 22.5 eV to 110 eV deg at 5 eV. It is obviously important in using the reduced coordinates that the ion energy be accurately determined. As described in our earlier work,¹⁰ the energy analyzer used in the present work was accurately calibrated so that our most probable ion energies are known with an absolute uncertainty of less than 0.1 eV at all energies. The techniques used to calibrate the ion energy are not stated in the work of Lorents *et al.*,³ but the energy spread of the ion beam is given as 2 eV. If we assume that the actual energy in their experiments was about 2 eV higher than the nominal value at all energies (possibly due to the plasma potential in the ion source) and use the "corrected" energies to compute the reduced angle τ , their results are brought into excellent agreement with ours for both $\text{Ar}^+ - \text{Ar}$ and $\text{He}^+ - \text{He}$. While we cannot justify such a correction on the basis of data available, it would account for essentially all of the observed discrepancies in the location of the structure observed in the two sets of experiments.

The theoretical calculations of Gilbert and Wahl¹⁴ give a value for the dissociation energy of the $^2\Sigma_u^+$ state of Ar_2^+ of $D_e = 1.25$ eV, and Lorents and co-workers⁴ have shown that the theoretical potential predicts a value of $\tau = 116$ eV deg for the rainbow angle in reduced coordinates. Assuming that the position of the rainbow angle in reduced coordinates is linearly related to the depth of the potential well, our results imply a value for D_e

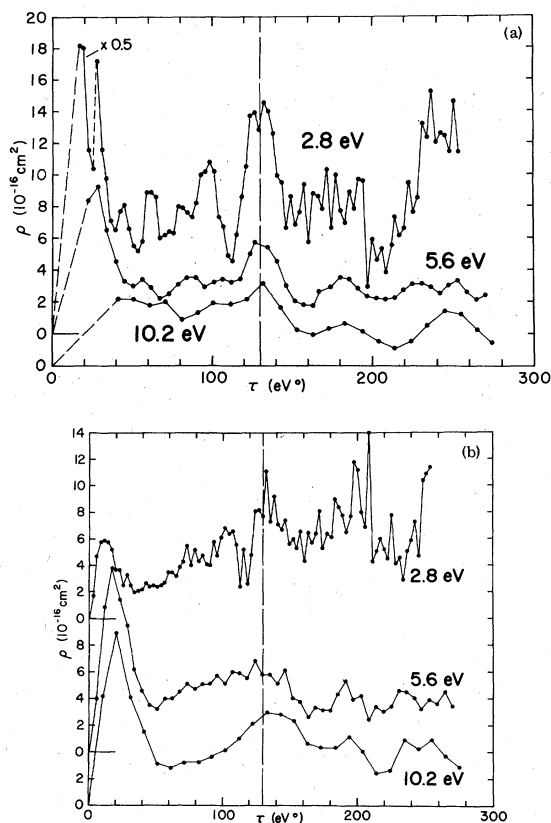


FIG. 4. Present results in the region of rainbow scattering plotted using the reduced coordinates $\tau = E\chi$ and $\rho = 2\pi\chi \sin\chi d\sigma/d\Omega$. Part (a) gives the results in the "elastic" region, and part (b) gives the results in the charge-exchange region with χ replaced by $\pi - \chi$ in computing the reduced coordinates.

of 1.40 ± 0.05 eV. This result is in reasonable agreement with the earlier result $D_e = 1.34 \pm 0.1$ from scattering experiments by Mittmann and Weise⁵ and the very recent value of $D_0 = 1.33 \pm 0.02$ eV determined by Moseley and co-workers⁹ using the technique of laser photofragment spectroscopy, but is significantly higher than both the theoretical value¹⁴ and the experimental value of $D_0 = 1.23 \pm 0.02$ eV determined by Ng *et al.*⁶ from the photoionization threshold of Ar_2^+ . It should be noted that since the photoionization result depends on determining the threshold for producing Ar_2^+ by ionization of the Ar_2 Van der Waals dimer, it gives a reliable lower limit for the dissociation energy of Ar_2^+ but does not necessarily determine the actual value.

Partial cross sections obtained by integrating the differential data over selected angular regions are summarized in Table II. At the two higher energies, the absolute backward-scattering cross sections are about 30% smaller than earlier theoretical¹⁴ and experimental¹⁵ results on charge

exchange. This discrepancy is within our estimated absolute uncertainty, and may indicate that we have overestimated the concentration of argon in the seeded neutral beam. As in the case of $\text{He}^+ - \text{He}$,¹⁰ we find a dip in the charge-exchange cross section at lower energies and a decline in the charge-exchange cross section relative to the elastic-scattering cross section with decreasing energy.

At the higher relative translational energies investigated in this work, regular oscillations in the differential cross sections are observed at scattering angles larger than the rainbow angle. The period and amplitude of these oscillations are in good agreement with the earlier results of both Aberth and Lorents³ and those of Mittmann and Weise⁵ at comparable translational energies. The latter investigators and Jones *et al.*¹⁶ have interpreted these oscillations as being due to gerade-ungerade (g-u) interferences involving the π states. The present results appear to contradict this interpretation since the g-u interference structure is expected to be antisymmetric about $\frac{1}{2}\pi$, while, as shown in Fig. 5, the regular oscillations in our results are symmetric. While some antisymmetric structure is visible in Fig. 5, particularly at larger scattering angles, the regular oscillations between 15° and 45° are very nearly identical in the forward and backward regions. This observed symmetry seems to imply that this regular structure is due to nuclear symmetry interferences rather than the g-u interferences as previously assumed.⁵

There is also apparent in our results, as illustrated in Fig. 5, a more slowly varying oscil-

TABLE II. Summary of partial scattering cross sections for $\text{Ar}^+ - \text{Ar}$ collisions.^a

T_R (eV)	σ_{CE}^b	σ_{El}^c	σ_6^d	σ_{174}^e	σ_{16}^f	σ_{164}^g
10.2	29.6	10.0	8.1	10.2	4.6	5.7
5.6	31.0	14.3	10.3	12.2	6.4	7.5
2.8	21.3	36.4 ^h	36.4	12.7	14.6	9.4
1.35	39.7	57.7 ⁱ	...	29	57.7	23.5

^a All cross sections in units of 10^{-16} cm².

^b Total "charge exchange" cross sections were obtained by integrating the experimental differential cross sections from $\chi = 90^\circ$ to $\chi = 180^\circ$.

^c Total cross section for elastic scattering between χ_{min} and 90° , for the two higher energies $\chi_{\text{min}} = 4^\circ$.

^d $\chi_{\text{min}} = 6^\circ$, $\chi_{\text{max}} = 90^\circ$.

^e $\chi_{\text{min}} = 90^\circ$, $\chi_{\text{max}} = 174^\circ$.

^f $\chi_{\text{min}} = 16^\circ$, $\chi_{\text{max}} = 90^\circ$.

^g $\chi_{\text{min}} = 90^\circ$, $\chi_{\text{max}} = 164^\circ$.

^h $\chi_{\text{min}} = 6^\circ$.

ⁱ $\chi_{\text{min}} = 16^\circ$.

^j Not determined.

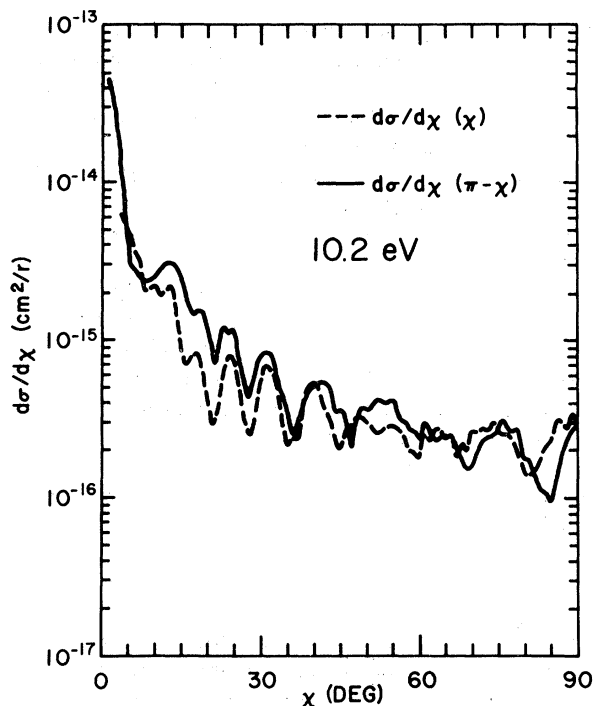


FIG. 5. Comparison of Ar^+ -Ar experimental differential cross sections $d\sigma/d\chi = 2\pi \sin\chi d\sigma/d\Omega$ corresponding to forward scattering (dashed line) and backward scattering (solid line) for a relative translational energy of 10.2 eV.

lation which is antisymmetric. In an attempt to extract this structure from the data we have computed the upper limit on the probability of charge exchange according to the formula

$$P_{\text{CE}} = d\sigma(\pi - \chi) / [d\sigma(\chi) + d\sigma(\pi - \chi)] \quad (2)$$

and have smoothed the result by taking a 5° running average of the data to remove the finer oscillations. The results are summarized in Fig. 6. The frequency of the slowly varying oscillation decreases markedly with decreasing collision energy, and, as in the case of He^+ -He collisions, the probability of charge exchange tends toward a maximum at small scattering angles for the higher energies, but at lower energies the probability for charge exchange appears to approach zero at small scattering angles.

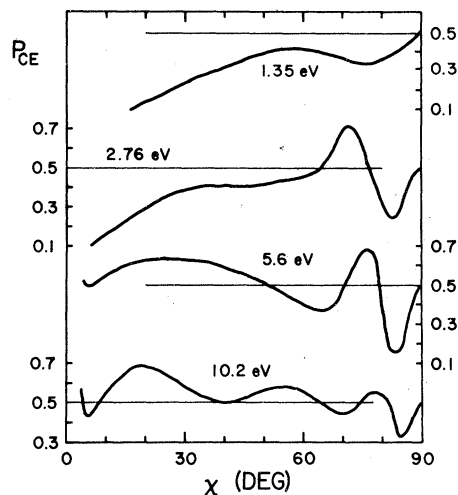


FIG. 6. Upper limit on probability of charge exchange P_{CE} as a function of scattering angle calculated from the experimental data according to Eq. (2) and smoothed by taking a running average of the data over a 5° interval to remove the final oscillations. The relative translational energy corresponding to each curve is indicated on the drawing and the correct scale for each is identified by the horizontal line at $P_{\text{CE}} = 0.5$ which intersects the curve.

IV. SUMMARY

The present results should contain sufficient information to determine accurately the Ar_2^+ potentials over a substantial range of internuclear distances by use of iterative inversion techniques such as those described by Olson and Mueller.¹⁷ However, such an inversion procedure presents a rather formidable task because of the number of potential curves involved and the presence of several overlapping interference patterns. Clearly, measurements such as those reported in this work, but employing different isotopes, would substantially simplify the interpretation since the g-u interference could be observed without the overlapping interferences due to nuclear symmetry.

ACKNOWLEDGMENT

This research was supported by the Donors of the Petroleum Research Fund, which is administered by the American Chemical Society.

*Present address: Dept. of Chemistry, Univ. of Houston, Houston, Tex. 77004.

¹For a recent review see C. K. Rhodes, *J. Quantum Electron.* **10**, 153 (1974).

²R. S. Mulliken, *J. Chem. Phys.* **52**, 5170 (1970).

³W. Aberthand D. C. Lorents, *Phys. Rev.* **144**, 109

(1966).

⁴D. C. Lorents, R. E. Olson, and G. M. Conklin, *Chem. Phys. Lett.* **20**, 589 (1973).

⁵H. U. Mittmann and H. P. Weise, *Z. Naturforsch. A* **29**, 400 (1974).

⁶C. Y. Ng, D. J. Trevor, B. H. Mahan, and Y. T. Lee,

- J. Chem. Phys. 66, 446 (1977).
- ⁷T. M. Millter, J. H. Ling, R. P. Saxon, and J. T. Moseley, Phys. Rev. A13, 2171 (1976).
- ⁸M. L. Vestal and G. H. Mauclaire, Chem. Phys. Lett. 43, 449 (1976).
- ⁹J. T. Moseley, R. P. Saxon, B. A. Huber, P. C. Cosby, R. Abouaf, and M. Tadjeddine, J. Chem. Phys. 67, 1659 (1977).
- ¹⁰M. L. Vestal, C. R. Blakley, and J. H. Futrell, preceding paper, Phys. Rev. A 17, 1321 (1978).
- ¹¹J. B. Anderson, R. P. Andres, and J. B. Fenn, in *Molecular Beams, Advances in Chemical Physics*, edited by J. Ross (Interscience, New York, 1966), Vol. 10, Chap. 8.
- ¹²The width of the measured energy distribution is approximately equal to the square root of the sum of the squares of the actual distribution and the analyzer transmission function; thus, at this energy, the analyzer transmission function broadens the measured distribution by only about 0.01 eV.
- ¹³D. C. Lorentz and W. Aberth, Phys. Rev. 139, A1017 (1965).
- ¹⁴D. Rapp and W. E. Francis, J. Chem. Phys. 37, 2631 (1962).
- ¹⁵R. F. Potter, J. Chem. Phys. 22, 974 (1954); W. H. Cramer, *ibid.* 30, 641 (1959).
- ¹⁶P. R. Jones, G. M. Conklin, D. C. Lorents, and R. F. Olson, Phys. Rev. A 10, 102 (1974).
- ¹⁷R. E. Olson and C. R. Mueller, J. Chem. Phys. 46, 3810 (1967).